

## **COMPREHENSIVE COMPUTER AIDED WIND DESIGN FOR ARBITRARY LONG SPAN BRIDGES**

**Dorian Janjic<sup>\*</sup>, Johann Stampler and Andreas Domaingo**

TDV Technische Datenverarbeitung GmbH/Bentley Systems

Gleisdorfer Gasse 5, 8010 Graz, Austria

E-mail: office@tdv.at

**Keywords:** Wind design, CFD, vortex method, flutter, galloping.

### **ABSTRACT**

This paper summarises theoretical models for the aerodynamic investigation of long span bridges. The discrete vortex method (DVM) is applied to solve the Navier-Stokes equations which describe the air-flow around bridges. Several wind design checks are discussed, ranging from one degree-of-freedom stability checks to the determination of critical wind velocities for classical flutter. The numerical implementation into a bridge design software package is outlined and practical examples are presented.

### **1 INTRODUCTION**

Due to the increased amount of newly constructed suspension and cable stayed bridges with extremely long spans all over the world, advanced wind design becomes more and more an issue of high importance. During the last century a couple of distinct aerodynamic phenomena have been observed and investigated for such bridges [1, 2]. Long span bridges are susceptible to wind induced vibrations and resulting damage mainly for two reasons: the long spans resemble more and more guitar chords with the according vibration properties; and the slender cross sections display in the worst case an airfoil-like behaviour. Therefore sophisticated wind design considerations in the design phase of such bridges are a must to estimate the risks and maximize safety.

Bridge engineering and design with regard to static and dynamic properties is nowadays almost entirely performed virtually on computers (e.g. [3]). But while methods to calculate the static of bridges, e.g. FEM calculations, are well established and widely used, investigation methods for dynamic wind influence are a state-of-the-art but not yet common topic. They provide valuable additional information to the well trusted wind tunnel measurements but have are not yet considered as stand-alone tools. One reason is that there are no all-in one solutions available, i.e. there are only methods which cover a part of the overall analysis. Good tool are available for the characterization of the air flow around bridge decks [4, 5]. The full 3D flutter equations have been solved in [6]. In this paper we present methods to combine all necessary steps for a comprehensive wind design analysis into one software package.

The first step is to investigate the air flow around the involved cross sections. In this context the main deck cross section is of highest importance, but also wake phenomena of double legged pylons may play a role. The temporal evolution of the flow is governed by the Navier-Stokes equations and a discrete vortex method (DVM) [7] is applied to find numerical solutions. For different flow situations different characteristic values can be derived which are used in the following to investigate divergence and stability phenomena and corresponding critical wind velocities. The problems discussed in this paper include galloping, torsional divergence and flutter instabilities. Examples of the application of the presented design criteria to practical problems (Hardanger and Storebælt bridge) will be outlined.

## 2 WIND LOAD AND AERODYNAMIC COEFFICIENTS

When a bridge is exposed to an oncoming wind flow, it will experience forces and overturning moments due to the wind pressure. In aerodynamics it is common to relate wind forces to the wind direction (cf. Figure 1), where the drag force  $f_d$  acts along and the lift force  $f_l$  perpendicular to the wind direction.

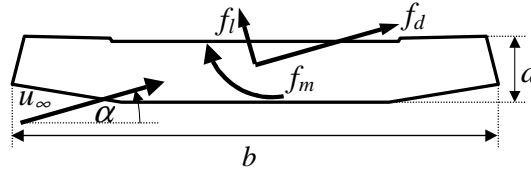


Figure 1. Definition of wind direction and aerodynamic forces.

The time averaged forces (marked with a subscript  $s$  hereinafter) on a fixed cross section are commonly expressed by the steady state aerodynamic coefficients  $c_d$ ,  $c_l$  and  $c_m$  via

$$f_{d,s} = \frac{1}{2} \rho u_\infty^2 \ell_d c_d \quad f_{l,s} = \frac{1}{2} \rho u_\infty^2 \ell_l c_l \quad f_{m,s} = \frac{1}{2} \rho u_\infty^2 a c_m \quad (1)$$

In the above equations it should be noted that the forces are given per meter of span length. The mass density of air is denoted by  $\rho$ , and  $\ell_d$ ,  $\ell_l$  and  $a$  are normalisation lengths and areas, respectively. In bridge engineering it is common to relate the normalisation for lift and moment to the width  $b$  of the cross section:  $\ell_l = b$  and  $a = b^2$ . The normalisation for drag is either related to cross section width  $b$  or height  $d$ .

In principle the steady state coefficients are dependent both on wind direction  $\alpha$  and velocity  $u_\infty$ . However the cross section used for bridges normally display less dependence on the velocity so that only the angle dependence is considered. The velocity is usually expressed in terms of the non-dimensional Reynolds number

$$\text{Re} = \frac{u_\infty b}{\nu} \quad (2)$$

where  $\nu$  is the kinematic viscosity of air, because if a model and the full scale cross section are considered at the same Reynolds number, the flows are equivalent. This fact is exploited in every wind tunnel measurement. However it must be noted that admissible Reynolds numbers in wind tunnels are of order  $10^5$ , while in reality  $\text{Re} > 10^7$ . Therefore an important preliminary for such tests is that the steady state coefficients is the previous assumption of Reynolds number independency next to several other similarity requirements[1, 8].

The time dependent lift and moment forces (with subscript  $t$ ) for oscillating cross sections are expressed by the so called flutter derivatives  $a_i^*$  and  $h_i^*$  as suggested by Scanlan [1]. They relate the resulting forces to the vertical and torsional displacements  $h$  and  $\alpha$ , respectively, and their first derivatives with respect to time:

$$\begin{aligned} f_{l,t} &= \frac{1}{2} \rho u_\infty^2 \ell_l \left( kh_1^* \frac{\dot{h}}{u_\infty} + kh_2^* \frac{b\dot{\alpha}}{u_\infty} + k^2 h_3^* \alpha + k^2 h_4^* \frac{h}{b} \right) \\ f_{m,t} &= \frac{1}{2} \rho u_\infty^2 a \left( ka_1^* \frac{\dot{h}}{u_\infty} + ka_2^* \frac{b\dot{\alpha}}{u_\infty} + k^2 a_3^* \alpha + k^2 a_4^* \frac{h}{b} \right) \end{aligned} \quad (3)$$

The flutter derivatives are dependent on reduced frequency  $k = b\omega / u_\infty$  where  $\omega$  is the circular frequency of oscillation. It should be noted that due to historical reasons the quantities are given with inverse sign compared to the steady state coefficients, e.g. with positive sign of lift and heave in downward direction. In most practical cases the flutter derivatives are not given in dependence of  $k$ , but of the reduced velocity  $u_{red} = 2\pi / k$ .

### 3 WIND DESIGN CHECKS

The performed design checks cover different phenomena which have been studied in the framework of bluff body aerodynamics. Corresponding theoretical models to explain these phenomena are based on equations of motion of the body in which certain degrees of freedom are frozen and the acting forces are derived from the available aerodynamic coefficients. Normally, only heave  $h$  and torsion  $\alpha$  are considered as degrees of freedom and if it is assumed that the centre of mass coincides with the elastic centre, the governing equations are

$$\begin{aligned} m(\ddot{h} + 2\zeta_h \omega_h \dot{h} + \omega_h^2 h) &= f_l \\ m_\alpha(\ddot{\alpha} + 2\zeta_\alpha \omega_\alpha \dot{\alpha} + \omega_\alpha^2 \alpha) &= f_m \end{aligned} \quad (4)$$

Mass and moment of inertia are given by  $m$  and  $m_\alpha$ , respectively. The natural circular frequencies are denoted by  $\omega_h$  and  $\omega_\alpha$ ,  $\zeta_h$  and  $\zeta_\alpha$  are the critical damping ratios. Driving aerodynamic forces are  $f_l$  and  $f_m$ . These structural can enter the calculation either as arbitrary additionally provided parameters, or they can be obtained from a preliminary Eigenmode calculation of the structural system.

#### 3.1 Galloping

According to [1], galloping is a low frequency oscillation in across-wind direction. Therefore, the aerodynamic forces can still be derived from steady-state coefficients, but the motion of the cross section causes a varying relative wind velocity  $u_r$ , as illustrated in Figure 2.

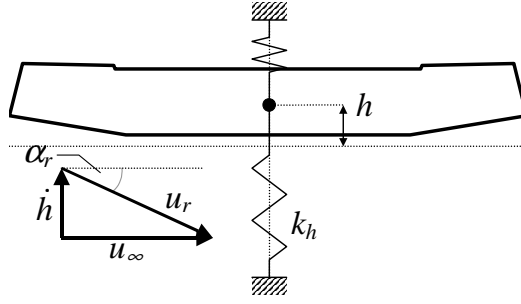


Figure 2. Relative velocity due to cross section heave in galloping case.

For low frequencies the approximation  $\dot{h} \ll u_\infty$  holds, and the drag and lift contributions along the heave direction can be estimated by

$$f_l \approx \frac{1}{2} \rho u_\infty^2 \ell_l \left[ c_{l0} - \frac{\dot{h}}{u_\infty} \left( c'_{l0} + \frac{\ell_d}{\ell_l} c_{d0} \right) \right] \quad (5)$$

The term in round brackets leads to an additional system damping and is known as the Glauert-Den Hartog criterion. Whenever this term becomes negative the system tends to an unstable solution. Since drag is always positive, galloping can only occur if the slope of lift is negative at  $\alpha = 0$ .

### 3.2 Torsional divergence

In many cases the moment coefficient is a monotonically increasing function of the wind incident angle. This is obvious for flat-plate-like cross section, because for increasing angle more area is exposed to the oncoming wind which results in increased overturning moment. Consequently the following stability problem can be observed for cross sections as sketched in Figure 3: as reaction to an initial twisting moment, the cross section will experience some twisting which increases the attack angle. Therefore the twisting moment increases, and so on.

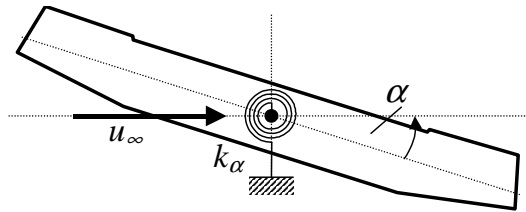


Figure 3. Mounting of cross section for torsional divergence problem

As long as the wind velocity is below some critical velocity, an equilibrium can be found at which twisting and reactive moment are equal. If the momentum is linearised around zero attack angle, this equilibrium is given by

$$k_\alpha \alpha = \frac{1}{2} \rho u_\infty^2 a (c_{m0} + c'_{m0} \alpha) \quad (6)$$

A stable solution for the deflection  $\alpha$  to this equation can only be found if

$$u_\infty < u_{c,\text{div}} = \sqrt{\frac{2k_\alpha}{\rho a c'_{m0}}} \quad (7)$$

In engineering applications it is common to express the torsional stiffness via the circular frequency and moment of inertia via  $k_\alpha = m_\alpha \omega_\alpha^2$ .

### 3.3 Classical flutter

In the case of classical flutter, a coupling of the two equations of motion (4) is observed. According to the wind velocity a small oscillation due to an initial disturbance leads to decaying, stable or sustained oscillations at a common frequency and a phase shift depending on the flutter derivatives. The critical wind velocity is again the velocity of transition from damped to sustained solution. It is calculated by following the method presented in [1, 9].

Since at critical wind velocity the solution must be an undamped oscillation, an ansatz  $(h, \alpha) = (h_0, \alpha_0) \exp(i\omega t)$  with  $\omega \in \mathbb{R}$  can be chosen. By inserting this ansatz into the equations of motion (4) with the aeroelastic forces (3), a linear system  $\mathbf{M} \cdot (h_0, \alpha_0) = 0$  is obtained. This system has non-trivial solutions only if the determinant of the coefficient matrix vanishes. Because of the used ansatz, the matrix coefficients are complex numbers and the determinant evaluates to a polynomial of fourth order in  $\omega$ . By considering the real and imaginary part of this equation separately, which is possible because the frequency is real, two real polynomials of fourth and third order are established:

$$\det(\mathbf{M}) = P_4(\omega; k) \equiv P_4^r(\omega; k) + iP_3^i(\omega; k) \quad (8)$$

The coefficients of these polynomials depend on  $k$  via the involved flutter derivatives, and a common solution to both polynomials to fulfil  $\det(\mathbf{M}) = 0$  is only possible for certain values of the reduced frequency  $k$  as indicated in Figure 4. Once such values for the reduced frequency  $k_{\text{crit}}$  and frequency  $\omega_{\text{crit}}$  have been found, the critical velocity can be calculated directly from the definition of the reduced frequency.

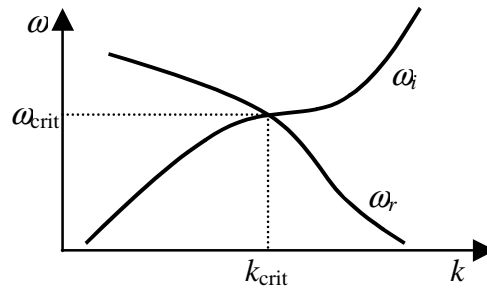


Figure 4. Solutions to the polynomials  $P_4^r$  and  $P_3^i$  and common solution for flutter problem

### 3.4 Single degree of freedom torsional flutter

For certain types of cross sections the flutter coefficient  $a_2^*$  becomes positive. In this case unstable solutions to the flutter equations are possible even if no coupling occurs. The single degree of freedom equation of motion for twist is then given by

$$m_\alpha (\ddot{\alpha} + d_{\text{tot}} \dot{\alpha} + \omega_{\text{tot}}^2 \alpha) = 0 \quad \text{with} \quad \begin{aligned} d_{\text{tot}} &= 2\zeta_\alpha \omega_\alpha - \frac{\rho u_\infty k a b a_2^*}{2m_\alpha} \\ \omega_{\text{tot}}^2 &= \omega_\alpha^2 - \frac{\rho u_\infty^2 k^2 a a_3^*}{2m_\alpha} \end{aligned} \quad (9)$$

For bridge deck sections the moment of inertia is usually high enough so that the resonant frequency  $\omega_{\text{tot}}$  is almost the same as  $\omega_\alpha$  of the undisturbed system. Therefore the reduced frequency can be approximated by  $k \approx b\omega_\alpha / u_\infty$  in the above equation. The critical point is at the transition from damped to sustained oscillation with  $d_{\text{tot}} = 0$  which happens for a critical flutter coefficient  $a_{2,c}^*$ . This implies a critical reduced frequency  $k_c$  from which the critical velocity can be calculated:

$$a_{2,c}^* = \frac{4\zeta_\alpha m_\alpha}{\rho b^2 a} \Rightarrow k_c \Rightarrow u_{c,t} = \frac{b\omega_\alpha}{k_c} \quad (10)$$

#### 4 DISCRETE VORTEX METHOD

The temporal evolution of air flow around a two dimensional bluff body like a bridge deck cross section can be described by the Navier-Stokes equations. If the air is assumed to be incompressible and of constant viscosity at a fixed temperature an equivalent description is provided by considering vorticity  $\omega = \nabla \times \mathbf{u}$ , where  $\mathbf{u}$  denotes the velocity vector. Its temporal behaviour is governed by the so called vorticity transport equation

$$\frac{\partial \omega}{\partial t} + (\mathbf{u} \cdot \nabla) \omega = \nu \nabla^2 \mathbf{u} \quad (11)$$

Due to the assumed constant density the continuity equation  $\nabla \cdot \mathbf{u} = 0$  must hold. The system is closed by the Biot-Savart relation to reconstruct velocity from vorticity:

$$\mathbf{u}(\mathbf{x}) = \mathbf{u}_\infty - \frac{1}{2\pi} \int \frac{\omega(\mathbf{x}') \times (\mathbf{x}' - \mathbf{x})}{|\mathbf{x}' - \mathbf{x}|^2} d\mathbf{x}' \quad (12)$$

where  $\mathbf{u}_\infty$  is the prescribed onset flow.

First attempts to solve these system of equations numerically were attempted in the field of aeronautics (e.g. [10]). The basic idea of the Discrete Vortex Method is to represent the vorticity field  $\omega(\mathbf{x})$  by a large number of vortex particles of a given size  $\sigma$  according to

$$\omega(\mathbf{x}) = \sum_i \delta_\sigma(\mathbf{x} - \mathbf{x}_i) \Gamma_i \quad (13)$$

where  $\Gamma_i$  is the total circulation of the vortex particle and the core function  $\delta_\sigma$  describes the shape of the vortex. Commonly the core function is a Dirac delta like function like a Gaussian distribution. By introduction this simplification the Biot-Savart integral collapses to a  $n \times n$  particle interaction. In order to establish an efficient numerical evaluation, sophisticated algorithms must be applied: lumping and vortex in cell methods [11], the so called P<sup>3</sup>M method [4] or the adaptive multipole algorithm [9, 12]. The latter one is also used in the present case.

Additionally to the determination of the velocity within the fluid domain, specific boundary conditions must be applied along the cross section outline. By imposing a surface vorticity layer determined by boundary element or Martensen method [7], either the no-penetration or no-slip boundary condition can be enforced. According to Walther and Larsen [13] it is sufficient to apply the no-penetration together with conservation of total circulation to fulfil the no-slip boundary condition implicitly.

Finally the time evolution of the vorticity field is integrated numerically by applying a fractional step method. In the first convection step, the second term on the left hand side of equation (11), the movement of the vortex particles along their characteristics within the velocity field is considered. The integration is performed in Lagrangian manner with a forward Euler discretisation. The diffusion term on the right hand side of the vorticity transport equation is treated with the random walk method suggested by Chorin [14]. Each particle is moved a randomly distributed distance into a random direction. For large numbers of particles this approach converges to the exact solution of the diffusion operator. Simultaneously to the diffusion of free vortices the vorticity bound in the layer next to the body outline is converted into nascent vortices and diffused into the flow.

The vorticity-flux created by the nascent vortices is also used to determine the time-dependent pressure distribution along the cross section outline up to an unknown datum value. By integrating the pressure along the surface time histories of force and moment are obtained. From these time traces the steady state coefficients are calculated straightforward in spite of their definition (1). To calculate the flutter derivatives either forced vertical or torsional oscillations are imposed on the cross section. The corresponding time histories of lift and moment can be compared with the theoretical ones, c.f. equation (3), with the methods discussed in [9] to yield the unknown coefficients.

**5 PRACTICAL EXAMPLES**

The first presented example is a CFD investigation of the steady state coefficients for the deck cross section of the Hardanger bridge in Norway. This suspension bridge with two traffic lanes and a cycle and pedestrian path will cross the fjord of same name in Norway. It will have a main span of 1310 m and a total length of 1380 m. The bridge towers will elevate to 186 m above sea level. The calculations were performed for a simplified cross section as indicated in Figure 5. The calculated steady state coefficients are presented in Figure 6.

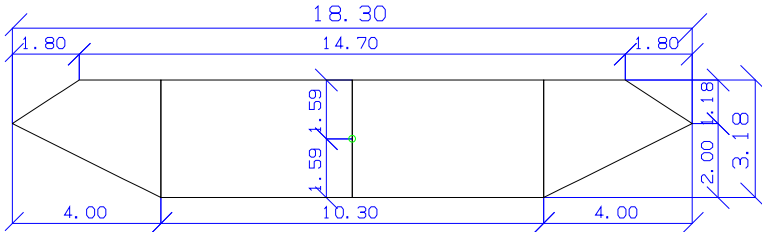


Figure 5. CFD cross section model for Hardanger bridge.

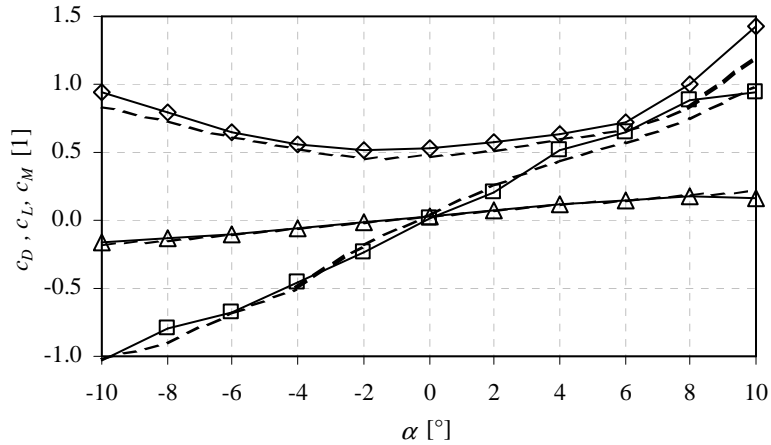


Figure 6. Steady state coefficients  $c_d$  ( $\diamond$ ),  $c_l$  ( $\Delta$ ) and  $c_m$  ( $\square$ ) of Hardanger bridge for  $Re = 5.5 \cdot 10^7$  (solid) and  $Re = 10^5$  (dashed).

The calculations were performed at full scale wind speed corresponding to a Reynolds number  $5.5 \cdot 10^7$  and at  $Re = 10^5$  which can usually be achieved in wind tunnels. Drag and lift show an average difference of 10% and moment of about 5% with a good qualitative coincidence. Therefore the assumption of Reynolds number independency is justified. The slope of the lift coefficient is positive for all considered wind directions which indicates that galloping will not occur.

Flutter investigations were performed for the Great Belt East bridge. This example is especially well documented both experimentally and numerical. The main cross section resembles that of the Hardanger bridge, but it is more stretched with a width of 32 m and a height of 4.3 m. The flutter derivatives calculated with the implemented DVM for  $Re = 10^5$  are shown in Figure 7 for the vertical coefficients  $h_i^*$  and in Figure 8 for the torsional coefficients  $a_i^*$ . A good agreement with numerical results obtained by Walther [9] is observed. The necessary structural data for the wind design checks according to [9] is given in Table 1.

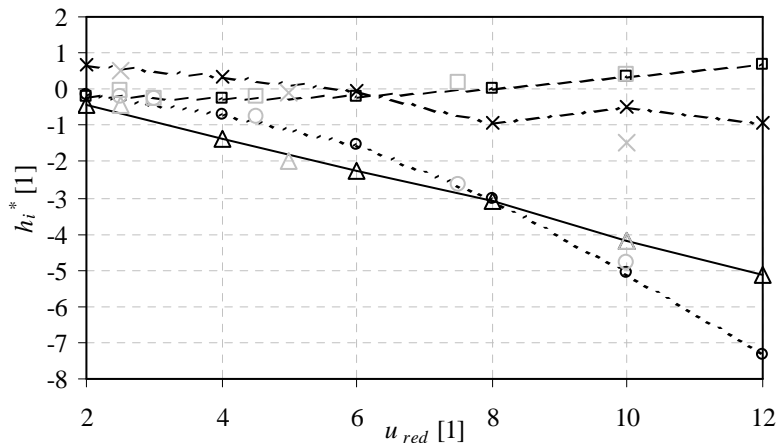


Figure 7. Flutter derivatives  $h_1^*$  ( $\Delta$ ),  $h_2^*$  ( $\square$ ),  $h_3^*$  ( $\circ$ ) and  $h_4^*$  ( $\times$ ) of Great Belt bridge. Results by Walther [9] are indicated by light symbols.

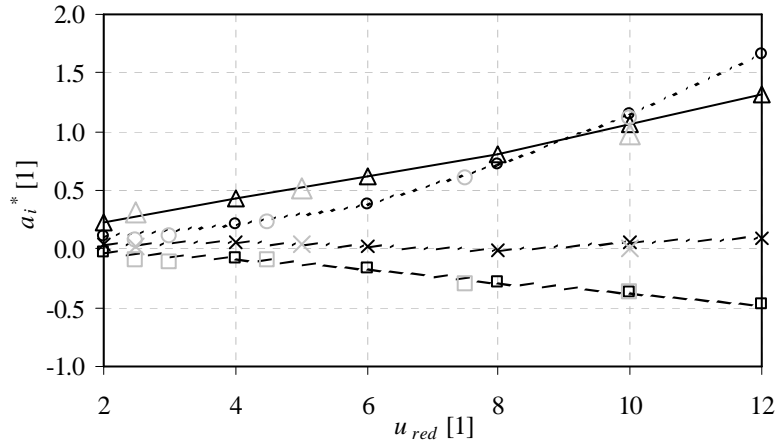


Figure 8. Flutter derivatives  $a_1^*$  ( $\Delta$ ),  $a_2^*$  ( $\square$ ),  $a_3^*$  (o) and  $a_4^*$  (x) of Great Belt bridge. Results by Walther [9] are indicated by light symbols.

$\rho$	$m$	$m_\alpha$	$\omega_h / 2\pi$	$\omega_\alpha / 2\pi$
kg/m <sup>3</sup>	kg/m	mg m	Hz	Hz
1.2	$17.8 \cdot 10^3$	$2.173 \cdot 10^6$	0.099	0.186

Table 1: Structural data for wind design check of Great Belt Bridge.

First it can be observed that the flutter coefficient  $a_2^*$  is negative for all reduced velocities. This implies that single degree of freedom torsional flutter is not possible. If an undamped system is assumed the critical velocity for classical flutter is 41.8 m/s. CFD calculations performed by Walther [9] result in 35.3 m/s and the evaluation based on flutter derivatives measured by Reinhold et al. [15] yields 37.6 m/s. This is an acceptable agreement. By increasing the critical structural damping to 0.5%, the critical flutter velocity is only slightly increased to 43 m/s.

## 6 CONCLUSIONS

This paper outlined the theoretical background of the necessary steps of wind design of long span bridges. To this end the overall process was spitted into the characterisation of the air flow and corresponding aerodynamic coefficients by means of the DVM. The second step was to evaluate the different design checks with the previously calculated coefficients. Several tests for the steady state coefficients predicted a good applicability for the full scale model. Comparisons of the flutter prognosis with wind tunnel test as well as numerical simulations showed a good agreement.

The overall analysis was performed within one software package. The advantage of this approach was that the same cross sections can be used as basis for the structural analysis and the CFD calculation. Moreover, the data exchange between different analysis tasks was simplified and accelerated. Thus the application of such an all-in-one solution significantly improves the efficiency of design tools for long span bridges.

## REFERENCES

- [1] E. Simiu, R. H. Scanlan, *Wind Effects on Structures*, third edition, John Wiley & Sons, New York, 1996.

- [2] E. N. Strømmen, *Theory of Bridge Aerodynamics*, Springer Verlag, Berlin Heidelberg, 2006.
- [3] *RM2006 User Guide and Technical Description*, TDV, Graz, 2007.
- [4] G. Morgenthal, *Aerodynamic Analysis of Structures Using High-resolution Vortex Particle Methods*, PhD Thesis, University of Cambridge, Cambridge, 2002.
- [5] A. Larsen, J. H. Walther, Discrete vortex simulation of flow around five generic bridge deck sections. *J. Wind Eng. Ind. Aerodyn.* 77 & 78, 591-602, 1998.
- [6] X. G. Hua, Z. Q. Chen, Y. Q. Ni, J. M. Ko, Flutter analysis of long-span bridges using ANSYS. *Wind and Structures.* 10, 61-82, 2007.
- [7] R. I. Lewis, *Vortex Element Methods for Fluid Dynamic Analysis of Engineering Systems*, Cambridge University Press, Cambridge, 1991.
- [8] H. Tanaka, Similitude and modelling in bridge aerodynamics, A. Larsen ed. *Aerodynamics of Large Bridges*, Balkena, Rotterdam, 1992.
- [9] J. H. Walther, *Discrete Vortex Method for Two-Dimensional Flow past Bodies of Arbitrary Shape Undergoing Prescribed Rotary and Translational Motion*, PhD Thesis, Technical University of Denmark, Lyngby, 1994.
- [10] A. Leonard, Vortex Methods for Flow Simulation. *J. Comput. Phys.* 37, 289-335, 1980.
- [11] P. R. Spalart, *Vortex Methods for Separated Flows*, NASA TM 100068, NASA, 1988.
- [12] J. Carrier, L. Greengard, V. Rokhlin, A Fast Adaptive Multipole Algorithm for Particle Simulations, *SIAM J. Sci. Stat. Comput.* 9, 669-686, 1988.
- [13] J. H. Walther, A. Larsen, Two dimensional discrete vortex method for application to bluff body aerodynamics, *J. Wind Eng. Ind. Aerodyn.* 67 & 68, 183-193, 1997.
- [14] A. J. Chorin, Numerical study of slightly viscous flow, *F. Fluid Mech.* 57, 785-795, 1973.
- [15] T. A. Reinhold, M. Brinch, A. Damsgaard, Wind tunnel tests for the Great Belt Link. *Proc. First International Symposium on Aerodynamics of Large Bridges.* 255-267, 1992.